university of groningen / faculty of science and engineering

Design and Development of a Small-Scale Dry Power-Take-Off System for the Ocean Grazer

Author:
Mark Immenga
S4916476

Supervisors:
A. (Antonis) Vakis, Prof
M. (Mehran) Mohebbi
A. (Andreas) Asiikkis

BSc Industrial Engineering and Management

Bachelor Integration Project
University of Groningen
June 27, 2024

Abstract

This research presents the design and development of a small-scale power take-off (PTO) system for wave energy converters (WECs). The model addresses the need for numerical validation by Ocean Grazer B.V. and aims to enhance the performance and efficiency of full-scale WECs. The report details the incremental improvements realized during two design cycles and evaluates the performance of the final design through several experiments. The design decisions involved utilizing a combination of industrially available and off-the-shelf components, along with addressing the resulting complications. The system's performance was assessed using transducers that collected data simultaneously through a microcontroller board. The experimental outcomes were promising, showing a relatively constant voltage output. Sudden sequential decreases in voltage output were well explained by pressure measurements, and the required force to operate the PTO was manageable. Further research is needed to refine the regulation of the PTO's input and improve the floater design to ensure full functionality within the wave flume at the University of Groningen.

Contents

List of Figures

1 Introduction

The renewable energy sector is experiencing rapid innovations due to increasing demands from many people to transition away from polluting energy sources. The failure to make this transition could lead to catastrophic consequences for the environment globally, including increased sea levels, more frequent and severe droughts, floods, and more extreme weather conditions in general. The irregularities in supply and demand in the energy market is a challenge that is to overcome in this question. Many renewable energy sources utilize weather conditions to generate electricity, such as wind turbines and solar panels. Since these weather conditions are variable, renewable energy sources alone cannot provide a consistent and reliable energy supply without the assistance of supplementary technology (Stram 2016). The company Ocean Grazer BV aims to provide solutions to these issues through innovation in the offshore renewable energy sector.

Most recent innovations include the development of a new Wave Energy Converter (WEC) that is able to harvest the kinetic and potential energy associated with an ocean in motion through a system of point absorbers. At the core of the WEC lies a so-called Power Take-Off (PTO) system, which is able to convert the hydrodynamic motion of the WEC into usable mechanical and electrical energy (Peña-Sanchez, García-Violini, and Ringwood 2022). The discussed research focuses on the design and development of a scaled PTO. In the following passage, the knowledge gap is further explained and justified with relevant literature. Afterwards, an outline of the research will be presented.

2 Problem Analysis

In this section the problem is analysed and explained within its context to create a better understanding of the problem preparatory to finding a solution.

2.1 Problem Context

The PTO is one of the major components of a WEC and has a major influence on the performance and efficiency of the system. Furthermore, it also determines the main characteristics of the external design of the converter. Ocean Grazer BV is aiming for the next step in their designing process of the PTO. Although numerical models of the PTO system are available, experimental validation is yet to be executed. The aim of this research is to bridge this knowledge gap by designing and implementing a scaled-down, simplified version of a single PTO in order to perform extensive testing in the company's wave tank laboratory.
Recent researches have contributed to a new the state of the art, such as a multi-wave absorber platform design, where both wind and wave energy can be harvested in an efficient manner (McLean et al. 2023). The deliverable that this research shall provide is a scaled and generalized experimental setup from which such products can be developed further.

2.2 System Analysis

Similar projects have shown that many designs of PTO's are available and suitable for WEC's. In Figure 1, multiple possible options are shown, such as the hydraulic system (Henderson 2006), a pneumatic system (Takao, Setoguchi, et al. 2012), and a direct (mechanical or electrical) drive system (Shadman, Avalos, and Estefen 2021).

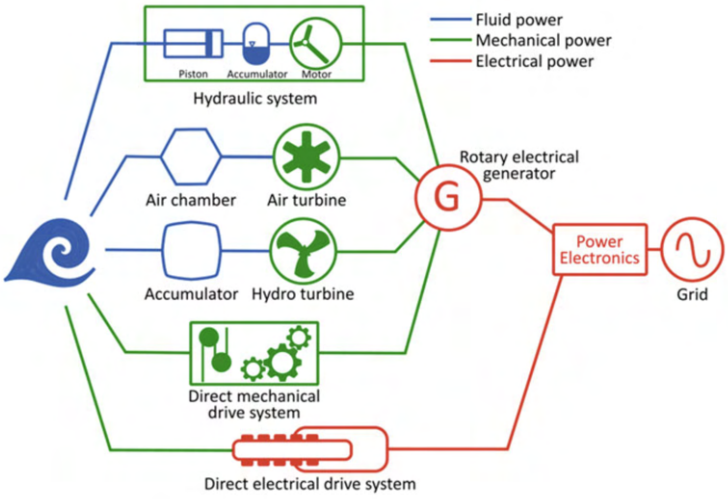

Figure 1: The five different PTO systems suitable to be implemented in a WEC, taken from (Têtu 2017).

Recent work in this project was focused on the hydraulic PTO system (Fernández Vuelta 2017), which will also be the starting point of this research. Hydraulic PTO's are known to be very suitable for turning wave energy into electricity, due to its capability of efficiently converting low frequency, high power waves (Jusoh et al. 2019). Nevertheless, the problem owner in this research, Prof. Antonis I. Vakis, is also open to other PTO forms when it is proven that these systems are more appropriate for the overall WEC design.

Figure 2: Example of a hydraulic PTO in a WEC.

Figure 3: Example of an air powered PTO in a WEC.

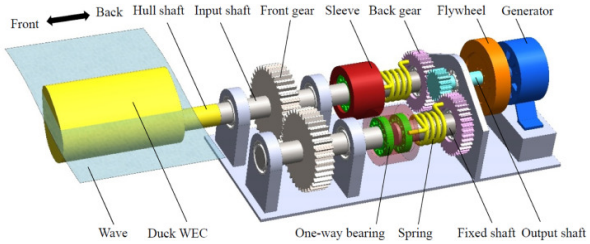

Figure 4: Example of direct-drive PTO in a WEC.

The hydraulic PTO system is powered by the mechanical motion of a point absorber that follows the wave dynamics. This drives a piston, also called the actuator, to pump hydraulic fluid within the PTO. The working principle of a hydraulic PTO system can be divided into two different groups: the variable-pressure concept and the constant-pressure concept (Penalba et al. 2017). In the variable-pressure system, a double-acting actuator is coupled to the hydraulic motor and generator directly, without the use of a rectification module. This makes the variable-pressure concept more simple and economic compared to the constant-pressure concept, which generally includes two or four check valves and two accumulators in order to provide more control within the system (Jusoh et al. 2019). The main function of the check valves is to control the direction of the fluid flow within the system, while the high-pressure (HP) and low-pressure (LP) accumulators smooth out the delivery of fluid by either providing or accumulating hydraulic flow to the motor. The specific design of the check valves is

important for the overall efficiency of the PTO as shown by (Hassink 2016).

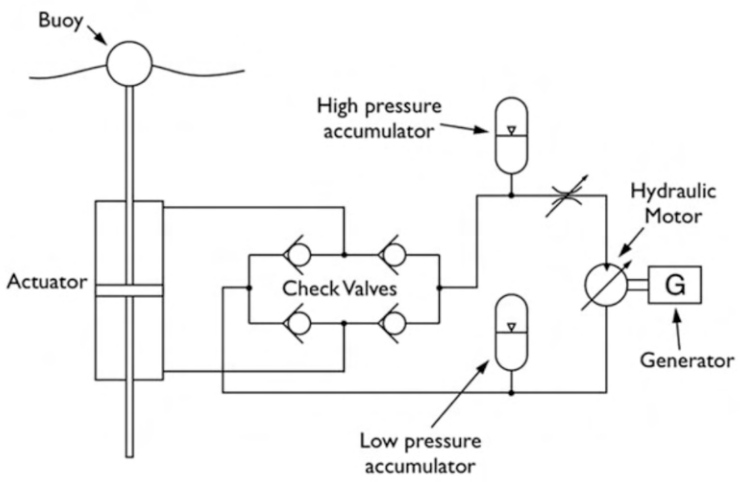

Figure 5: Schematic of the working principle of a hydraulic PTO making use of the constant-pressure concept. Taken from (Drew, Plummer, and Sahinkaya 2009).

In the upward movement of the double-acting actuator, highly pressurized fluid is forced through the inlet of hydraulic motor, which in turn drives the generator to deliver electricity to the grid. In the downward movement of the actuator, low pressure hydraulic fluid flows back to the cylinder. The conversion of fluid pressure into mechanical torque of the motor's shaft is described by the equation 1.

$$T_M = \alpha D_\omega \Delta P_M - T_{losses} \tag{1}$$

Where T_M is the torque generated by the motor, α is the motor displacement fraction, D_ω the displacement of the motor, δP_M is the pressure difference between the in- and outlet of the motor, and T_{losses} are all mechanical losses, such as friction.

2.3 Stakeholder analysis

The start-up company Ocean Grazer was founded in 2018 and is a spin-off from the University of Groningen which started the project together with drs. Wout Prins in 2014. The company is currently led by Frits Bliek (CEO) and Max Duursma (COO) and aims to "turn knowledge and intellectual property into commercial products"(*Home — oceangrazer.com* n.d.). In this challenge that is faced by the Ocean Grazer BV, multiple stakeholders are involved. Prof. Antonis I. Vakis, co-founder and scientific advisor of Ocean Grazer BV, is the problem owner in this research. Furthermore, the managing board of the company is another stakeholder. They lend a sympathetic ear and are highly interested in the research. Another key stakeholder

in the Ocean Grazer project is the University of Groningen, which demonstrated early belief in the initiative and provided essential support throughout its development. The stakeholders can be arranged on the basis on level of interest and power in a Mendelow's diagram as can be seen in Figure 6.

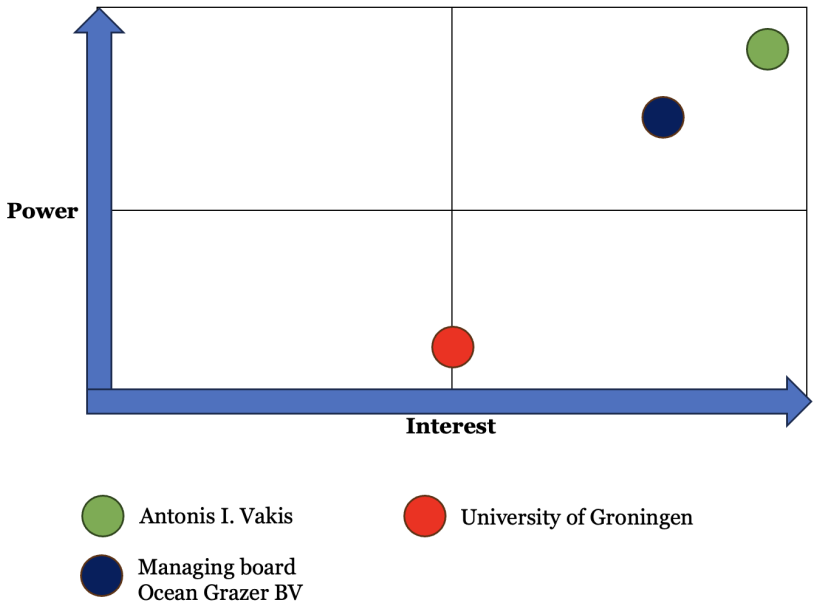

Figure 6: Mendelow's diagram categorizing the stakeholders into different levels of interest and power.

2.4 Problem statement

Although noticeable advancements have been made in the creation of numerical models regarding the Ocean Grazer's power take-off system, the absence of experimental validation is hindering the company from advancing its development of the wave energy converter.

2.5 Research Objective

The research objective is to design and develop a small scale hydraulic power take-off system for a wave energy converter and perform dry testing in order to validate numerical models of Ocean Grazer B.V. in a time frame of 3 months.

For this objective, the two-step SMART method has been utilized (Bjerke and Renger 2017). The first step is defining that the research objective is specific, measurable and relevant. The research is specifically focused on hydraulic PTO systems. The research is measurable, as several sensors should be able to measure the performance of the system. Furthermore, the research is especially relevant, as global warming issues may have catastrophic consequences in the near future. A positive outcome to this research will contribute to the feasibility of

renewable energy sources. The second step in designing a SMART research objective is to specify the attainability and the time span of the research. The time frame for this research is given to be 3 months. The research is attainable since it is reasonable to expect that both literary research and a generalized dry model can be finished within 3 months.

3 Research Design

3.1 Methodology

In this part of the report the overarching methods used to reach the goal of the research are presented. Wierenga's design and engineering cycles are used as a tool to provide a clear overview of implementation and design steps leading to the final deliverable (Wieringa and Moralı 2012).

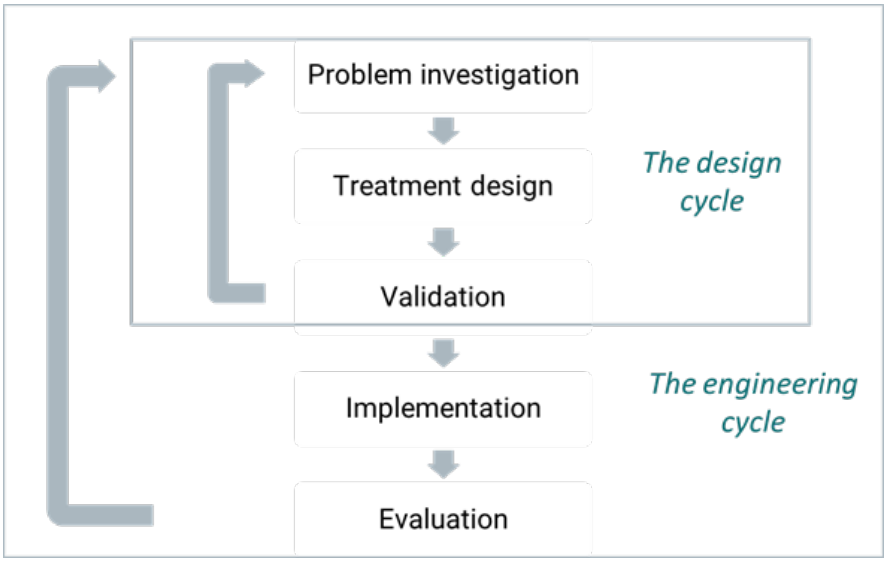

Figure 7: Wierenga's design and engineering cycle showing the different stages in designing a solution for an engineering related problem. Taken from (Wieringa and Moralı 2012).

3.2 Research Questions

Now that an overview of the different design steps is established, a set of research questions can be written.

Core question:
How can we design, develop and test a small scale hydraulic power take-off system for a wave energy converter for Ocean Grazer B.V.?

Sub-questions:
1. What are the current advancements made by comparable projects regarding hydraulic PTO's?

2. What are the functional requirements of the small-scale PTO, as requested by Ocean Grazer B.V.?

3. What combination of industrially available and off-the-shelf components are required to design a small-scale hydraulic PTO?

4. How can the experimental setup be tuned, such that it can be mounted in the wave tank of the University of Groningen?

3.3 Methods and Tools

Problem investigation:
In the first stage of this research, literary research must be done in order to gain a broader knowledge on the working principle of hydraulic PTO's. In order to achieve this goal, the evaluations of several recent WEC projects by similar institutes can be studied. At this stage of the research, it is crucial for the study to prioritize breadth, as obtaining a comprehensive understanding of the system is essential (Verschuren, Doorewaard, and Mellion 2010). Therefore, also non-hydraulic PTO systems can be examined to get to know the benefits and drawbacks of the available power take-off systems. This stage in the research aims to answer sub-question 1.
When a broader view of the problem is obtained, more depth focused desk research can be performed to find out the actual functional requirements of the artifact that is to be designed (sub-question 2). To answer this question, the exact purpose of the deliverable, and its compatibility for further studies must be established. Both stages of the problem investigation are qualitative research forms.

Treatment design:
In the second stage of the research the artifact will be theoretically designed. The functional requirements obtained in the previous stage stand at the base of this design. The treatment design is accomplished when a CAD design can be presented.

Validation:
In the last phase of the design cycle, the treatment design is validated using the functional requirements obtained in the first phase. A bill of materials (BOM) consisting of commercial off-the-shelf components is created to fit the design (sub-question 3). When the design fulfills all requirements, the research may proceed to the implementation stage. If the design is not satisfactory, the design cycle can be started over as shown in Figure 7.

Implementation:

Now that the theoretical design is finished, it can be implemented in the wave tank, located in the University of Groningen. In this tank, a large piston controlled by an electromotor moves through a long bath which has been specifically designed to simulate the wave dynamics of the ocean. Although the first model shall be tested outside of this wave tank, it is still useful to make use of the facilities in the workshop and have to opportunity to base certain mechanisms on earlier created artifacts. Assistance from the technicians of the laboratory is available in order to make the design technically viable.

Evaluation:
In this last stage of the engineering cycle, the developed artifact is evaluated based on an experiment. Transducers can be installed within the system to test several parameters, such as force, pressure, displacement and voltage. Afterward, solutions are sought for any issues that may have been encountered. The design cycle is then started over, as shown in Figure 7. In some instances, the evaluation of the engineering cycle may already serve as the problem investigation of the design cycle , such that the research can proceed to the treatment design phase directly (Wieringa and Moralı 2012).

3.4 Deliverable

The research and its execution will be part of the Bachelor Integration Project of the Industrial Engineering and Management Bachelor. The final deliverable consists of a generalized, simplified small-scale experimental model of a hydraulic power take-off system. Furthermore, a final report is written in which the design process is documented, which is due on the 25th of June. Lastly, a poster must be created showcasing the most important aspects and results of the research. The poster must be presented during the Symposium on the 27th of June.

3.5 Research Planning

The required time for the research is set to 12 weeks. It is expected that two engineering cycles can be performed in this time span, as described in 3.1. All elements of the engineering cycle are showcased in a histogram in Figure 8.

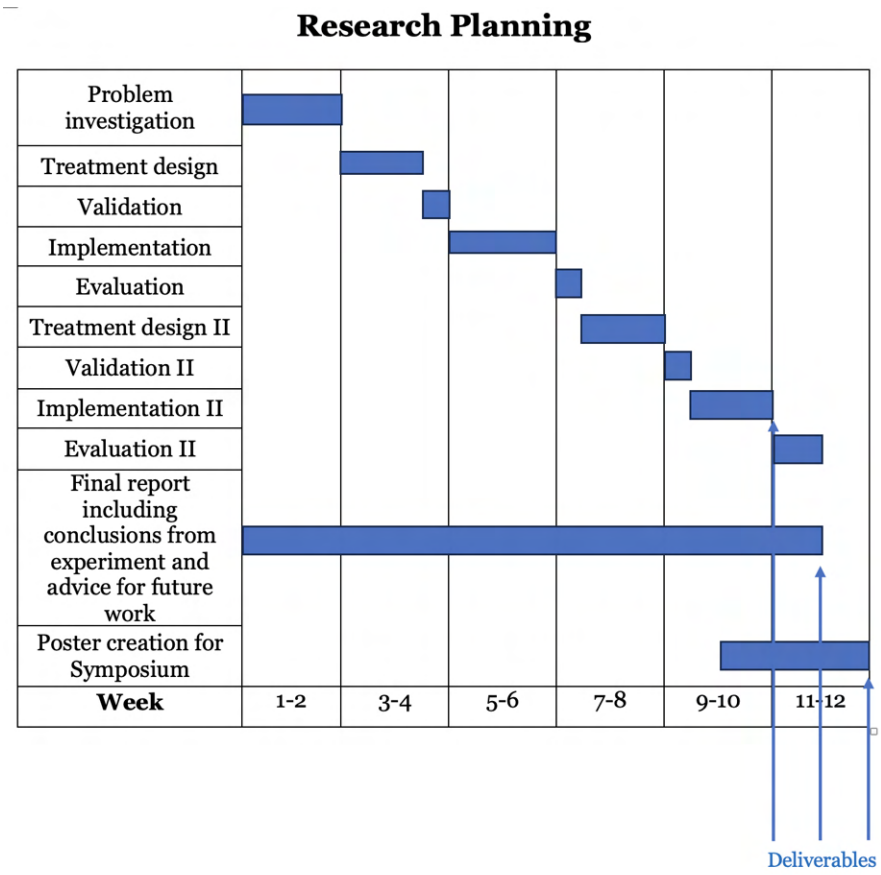

Figure 8: Histogram showing which activities must be executed in which week of the research. A partially parallel planning process is used in this research.

4 Theoretical Design

From the problem analysis, it was found that the hydraulic PTO system is most suitable for large-scale wave energy converters (Jusoh et al. 2019). Therefore, it is important that the small-scale deliverable of this project is able to simulate the results of the hydraulic PTO system.

In first instance, the possibilities for a fully hydraulic small-scale model have been explored, with only industrially available hydraulic components in the system. Following the article by Pedro Beirão and Cândida Malça (2011) , a bill of materials was made in order to make an inventory of the required parts.

Part name	Amount	Image
Double acting hydraulic cylinder	1	
Hydraulic motor + generator	1	
Check valves	4	
Throttling valve	1	
Low pressure accumulator	1	
High pressure accumulator	1	
Hydraulic hose	1	
Hose T split connection	11	

Figure 9: Bill of Materials (BoM) of the system

Following the bill of materials, a CAD (Computer Aided Design) model of the small-scale hydraulic PTO was constructed as shown in Figure 10, 11 and 12. The CAD software used was Onshape, and self made models were combined with readily available CAD models of off the shelf components from traceparts.com and grabcad.com to create the hydraulic circuit.

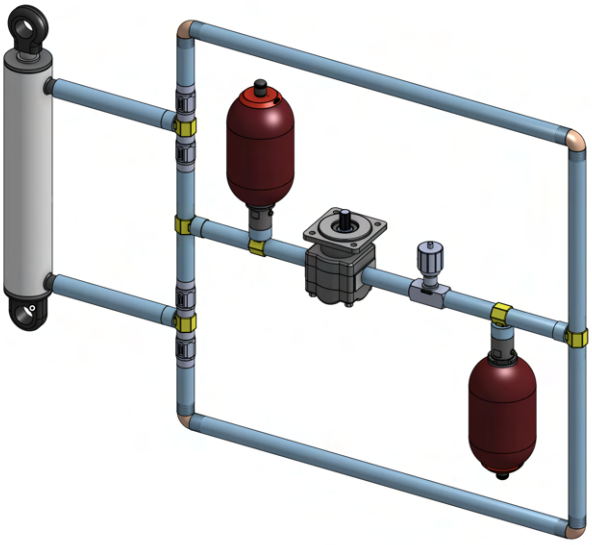

Figure 10: Isometric view of the CAD model of the hydraulic PTO.

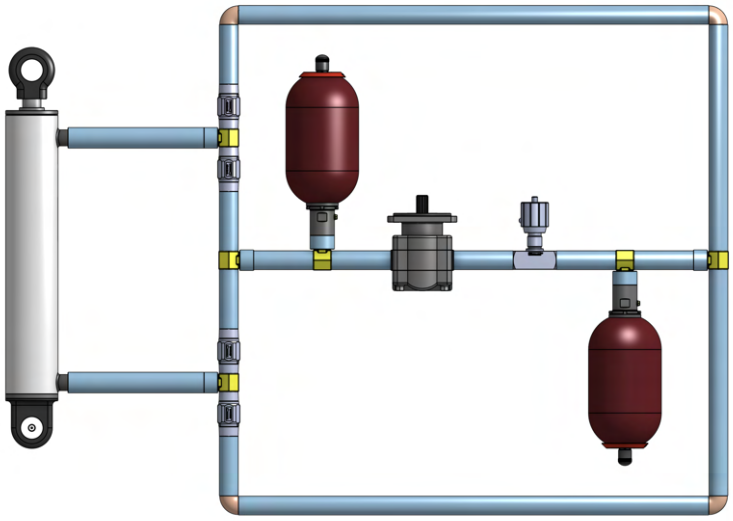

Figure 11: Front view of the CAD model of the hydraulic PTO.

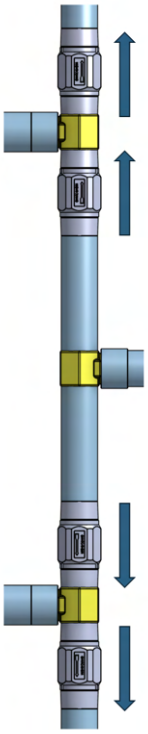

Figure 12: Close-up view of the check valve system.

In this system, the cylinder is being moved up and down through its connection with the buoy. When the buoy finds itself on a wave crest, the hydraulic cylinder goes into an upstroke, and the hydraulic fluid is forced through the upper outlet of the cylinder. This pressurizes the complete system, and due to the area of lower pressure below the piston, the fluid is forced back to the cylinder. Afterward, a wave trough forces the system to work in the other direction. A system of four check valves ensures that fluid is directed towards the inlet of the system, independent of the movement direction of the piston inside the cylinder. Figure 12 shows a close-up view of the check valve system.

The initial conditions for the system are determined by the buoys weight and the wave amplitude. After visiting the wave tank of the University of Groningen, it was found that the wave amplitude varies between 0 to 5 centimeter, meaning that the range of the cylinder should be 10 centimeter at least. The buoy that is used in the wave tank is a hollow cube constructed out of acrylic glass.

Figure 13: The wave flume in the University of Groningen

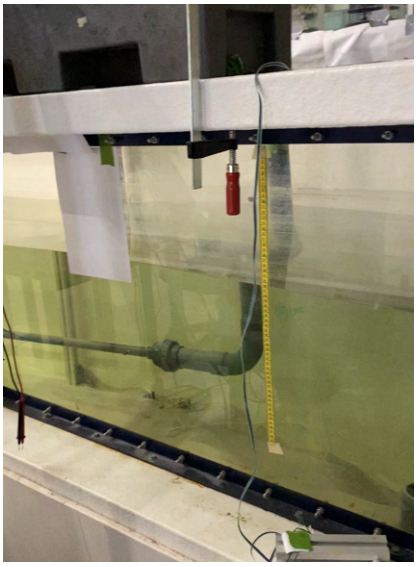

Figure 14: Measurement of the wave amplitude

Dutch industrial hydraulic stores Hydroliek24 and Hydraulicworld were contacted for consultation about the required components for the system. It was quickly concluded that general hydraulic components that are commonly used in industry are built for different purposes, with higher forces acting on the system. In a conversation with mr. R. Schouten from Hydraulicworld, it was found that a regular double acting hydraulic cylinder needs at least 3000 N of force to function properly. The floater that is constructed out of acrylic glass has a very low mass and will not have enough force to move this cylinder. Even when a new buoy of a higher mass of approximately 10 kilograms is constructed, which is estimated to be the maximum that is still realistic in this wave tank, approximately 100 N of force is acting on the cylinder in the downstroke due to gravitational forces. Still, this value is much lower than the

force that is required to get the system running. With a working pressure of around 180 bar, it can be concluded that the industrially available hydraulic components are designed for larger systems with higher forces.

Furthermore, the hydraulic motor's ideal RPM lies between 500 and 1000 rotations per minute. With a general efficiency of around 60 to 70 %, it will be a major challenge to get the motor running on these high RPM values, as this 30% efficiency lost must first be overcome.

Together with the supervisors of this project, alternative solutions were sought. In many other similar projects, non-hydraulic systems (such as direct drive) are used as described in Figure 1. However, these systems are not representative for the output of large-scale hydraulic PTO's. Therefore, the components of the small-scale hydraulic model must be chosen differently, such that they have a similar properties compared to the full-scale model.

5 Experimental Design

In this section, the construction phase of two prototypes will be elaborated.

5.1 Prototype 1

In consultation with mr. R. Schouten, other cylinder types have been investigated, such as pneumatic cylinders. These types of cylinders operate on smaller pressures, and also work with fluids, such as water or a mineral oil. This concept is promising, since these cylinders generally have operating pressure of 6 to 10 bar. However, it is still expected that the buoy in the wave tank will not have enough force to overcome the frictional forces within the pneumatic cylinder. Therefore, the first prototype must contain a cylinder that has minimal friction and a relatively large range.

After some research, it was found that there are several types of water toys available for children, that make use of a cylinder concept. These so-called 'piston pumpers' consist of four main parts: the cylinder, the piston, the opening and the handle. Children can absorb water into the cylinder by pulling back the handle, which creates a low pressure area in the cylinder. By pushing the handle back again, the water is forced through the small opening, which creates a small but powerful stream of water going out of the opening. There are several advantages to using this product in the PTO circuit as the main cylinder. Since the cylinder is a children's toy, it must be operated with minimal human force, meaning that the friction between the piston head and the cylinder must also be very low. Furthermore, with a length of 45 centimeters, the range is more than enough for this particular use case in the wave flume. The cylinder is constructed out of PET (polyethylene terephthalate), which is easily adaptable and strong enough for the relatively low pressures that are present in the small-scale system. This material would definitely not be suitable for a cylinder in a large-scale system, where much higher forces are present, and the conditions of the rough open sea negatively impact the plastic's quality.

Figure 15: A pneumatic cylinder from the brand Festo.

Figure 16: A 'piston pumper', used by children as a water toy.

The motor is the second major component of this system. Instead of a hydraulic motor that runs on hydraulic fluid and requires a high RPM to be efficient, a small-scale hydro generator can be used. The blades in this generator need much lower forces in order to turn, and additionally, electricity is easily generated with lower RPM values. The hydro generator produces a 12 Volt output when running consistently and has two 1/2" BSP outer thread connections.

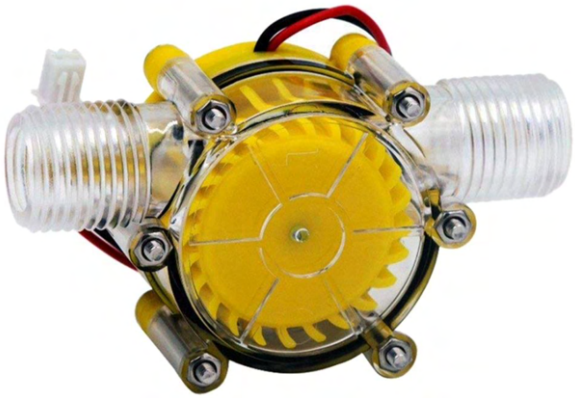

Figure 17: A turbine hydro generator that converts mechanical energy into electrical energy.

The different components within the system are connected by a hose. In the first prototype, a polyurethane (PU) hose was used with an inner diameter of 5 millimeter. This type of tubing is commonly used in pneumatics, making it well resistant against leakages. In order to connect the hose to the cylinder, two different adapters were designed in CAD software and created using additive manufacturing. The plastic opening of the cylinder was removed, leaving the cylinder open. The first 3D printed adapter was then slid on to the cylinder. The second adapter was fitted on top of the cylinder and included a cap to close the opening of the cylinder. Both adapters were featured with a printed 1/4" BSP thread, such that pneumatic

adapters could be easily fitted. The adapter was designed to fit on the cylinder very tightly to avoid leakage. Using a Dremel, two holes were created in the PET cylinder.

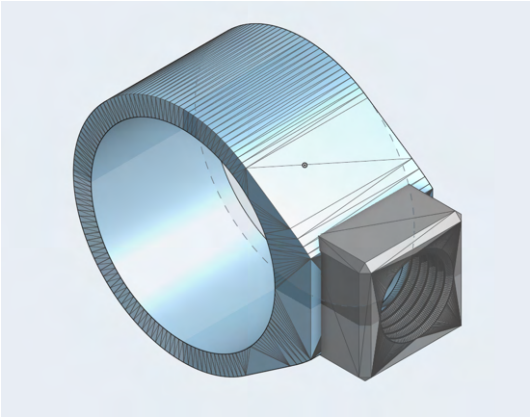

Figure 18: CAD model of the adapter that is fitted on the cylinder.

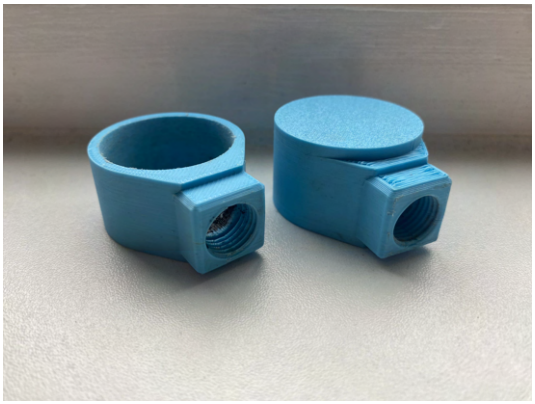

Figure 19: Two versions of the 3D printed adapter: one with cap and one without.

In order to assure the direction of flow within the system, a system of four check valves was used. The small check valves that were purchased for this small-scale PTO are normally used in aquaria to stop water from flowing into air pumps that are connected to devices that are located below the water level. The main function of these one-way valves in this system is to redirect the output water streams from both sides of the cylinder to one input into the hydro generator. This is crucial, as the generator is only able to rotate in one direction. Pneumatic push-in valves and T-connectors were used to connect the hosing to all components, since they are straight forward in usage and are not sensitive to leakages.

After connecting the main parts of this system, two challenges were yet to be solved:
1. Creating a water tight connection between the hydro generator and the pneumatic hose.
2. Sealing the piston opening without provoking large frictional forces.

With no readily available adapters to fix the pneumatic hose into the input and output connections of the hydro motor, a special cylindrical adapter was designed in CAD software. Using additive manufacturing, the adapters were printed using TPU (Thermoplastic Polyurethane) filament. This material has both the characteristics of rubber and plastics, imposing high ductility, durability and tensile strength (Xu et al. 2020). With its high flexibility, the adapter can be designed with negative tolerances, ensuring a perfectly tight and waterproof fit.

Since the cylinder is designed to have water below the piston's crown and air above the piston's skirt, an opening is present around the piston's rod to relief air when the piston is being pulled upon. Now that the cylinder is filled with water on both sides of the piston's

head, and separate holes have been created for the in- and output connections, this opening must be closed in such a way that no water is being able to escape, while not provoking large frictional forces upon the piston's rod. Large-scale systems generally utilize industrial piston seals, consisting of a combination of different materials and shapes to attain exactly these characteristics. However, in the small-scale system of this project, these seals still introduce friction figures well above the buoy's force limit. Therefore, a simple O-ring was used to seal the piston. A 3D printed adapter was created to keep this O-ring in place.

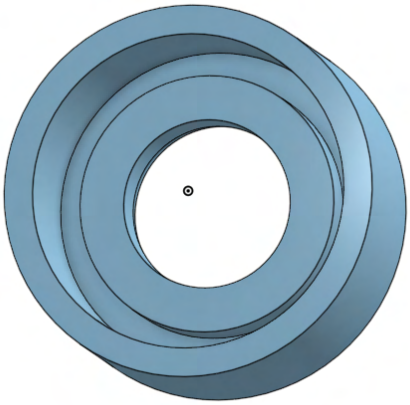

Figure 20: CAD model of the adapter that is used to keep the O-ring in place.

Figure 21: 3D printed adapter that is used to keep the O-ring in place.

In this first prototype, the accumulators have been left out of the system in order to keep the frictional losses at a minimum. Nevertheless, during the testing phase of the first prototype, several problems were observed:

1. Although the water was flowing in the right direction through the tubing, the hydro generator's turbine was rotating scarcely.
2. The human force required to move the piston was perceived to be significant.
3. Serious leakages appeared on the connection points of the piston.

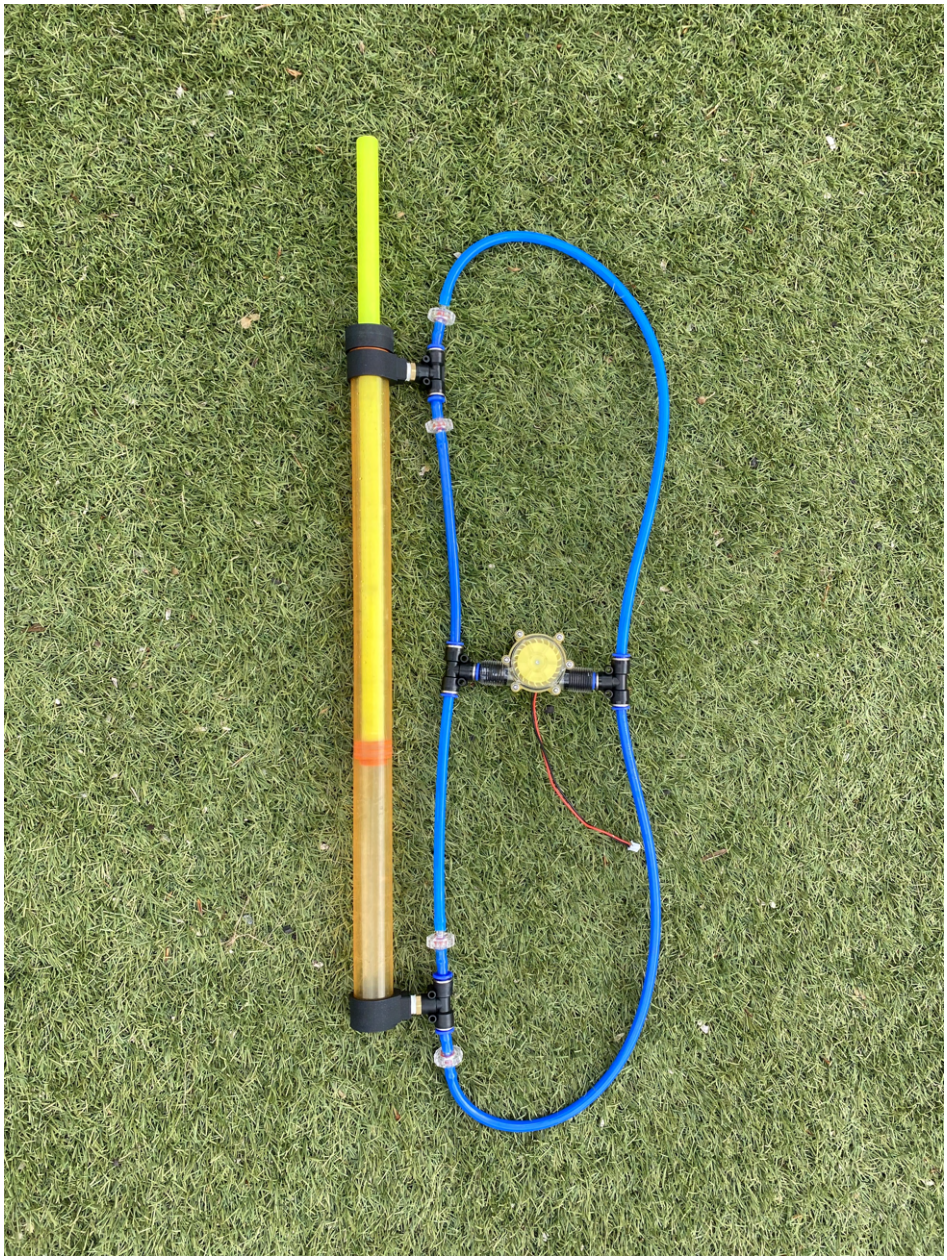

Figure 22: Top view of the first small-scale PTO prototype.

5.2 Prototype 2

In the second designing phase, these issues were to be resolved. The high force that was needed to move the piston was mainly caused by the high pressure that was present in the system. One of the check valves was tested outside of the system to observe its functioning, and it was found that although it did not let any water through in one direction as it should, the valve also reduced the flow in the order direction drastically. This obstruction in the flow throughout the system increased the pressure inside the system, and with that also increasing the occurrence of leakages at the fittings. Furthermore, the relatively small pneumatic tubing that was fitted caused the total losses to increase even further.

Bernouilli's law describes the relation between pressure, kinetic and potential energy in fluid systems. It is given by:

$$P + \frac{\rho}{2}v^2 + \rho gh = constant \tag{2}$$

It is of common belief that when fluid enters a tapering pipe, its pressure will increase. Bernouilli's law proves the contrary. When fluid particles move through a tapering hose, their velocity must increase in order to maintain a given flow rate. Bernouilli's principle states that the pressure inside a pipe is inversely proportional to the velocity of the fluid within that pipe.

More accurately, the energy losses of a fluid within a small pipe are greater. There are two main reasons for this phenomenon:
1. The ratio of the circumference of a circle ($2\pi r$) over its area (πr^2) as shown in equation 3 decreases as the pipe diameter becomes larger. This indicates that for larger pipes, the relative portion of water particles touching the walls of the pipe is smaller, thus reducing the the overall friction through the pipe.

$$\frac{Circumference}{Area} = \frac{2\pi r}{\pi r^2} = \frac{2}{r} \tag{3}$$

2. In order to maintain a given flow rate in a smaller diameter pipe, the velocity of the fluid flow must increase. A fluid that has a higher velocity generally is more turbulent, indicating it has a higher Reynolds number. High Reynolds numbers are associated with larger frictional losses (Nur, Afrianita, and Ramli 2019). Therefore, the main objective of the second design cycle was to reduce these energy losses as far as possible, such that the force needed to move the piston is reduced, and the hydro generator will rotate more easily. This goal should be accomplished by choosing more industrial, and larger scale components, along with some design changes.

First of all, the tubing was changed from a 5 mm pneumatic hose to a 13 mm hose that was designed for water applications. Larger and commonly available adapters could now be used to connect the system. For example, instead of using the self-manufactured TPU adapter to connect the tubing to the hydro generator, a threaded 1/2" BSP Gardena Tap Connector could be used. These parts are designed to withstand leakages when properly connected. Similar Gardena adapters were used to connect the hosing to the cylinder, together with two newly designed 3D printed adapters. One major design change was that the adapter that was fitted onto the head of the cylinder now also had its opening in the longitudinal direction of the cylinder. The small hole that was created on the side of the cylinder caused for an extra leakage point, which was unfavourable.

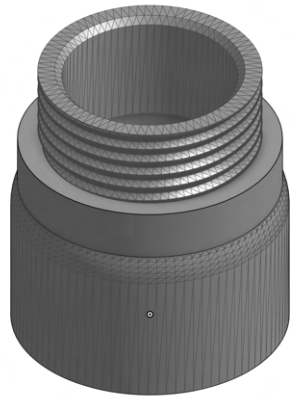

Figure 23: CAD model of the adapter that is used to keep the O-ring in place.

Figure 24: Updated 3D printed adapters with an integrated mounting plate.

Furthermore, the small check valves that produced high pressure levels within the systems were exchanged for much larger, industrially available check valves that fitted onto the 13 mm tubing. These one-way valves were physically tested to let fluid pass through one side without any increase of pressure in the system, while being shut off through the other direction.

The combination of all these improvements impacted the system in a positive manner, with the hydro motor now rotating during both the up- and downstroke. In addition, less force was required to move the piston up and down. After the second design was finished, a wooden construction was manufactured in order to keep it positioned firmly.

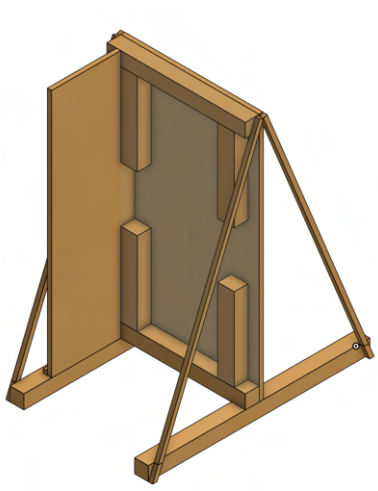

Figure 25: CAD model of the wooden construction that was designed to keep the PTO in place.

Figure 26: The finished wooden construction from the workplace.

Figure 27: The final design of the small-scale PTO mounted onto a wooden frame.

6 Experimental Setup

Initially, the small-scale PTO was intended to be tested inside the wave flume that is located in the Univerisity of Groningen. The wooden construction frame was especially designed to be positioned on the side walls of this wave tank. However, after some further observations, it was concluded that due to the lack of a floater that is suitable for this PTO, and a piston that would not be able to sustain the impact of the lateral forces following from the wave generation plate, installation would not be feasible.

In order to test the performance of the small-scale PTO that followed from the second design cycle, four different sensor types were integrated in the system, and dry testing was executed. The dynamics of the displacement of the piston, the required force, the pressure inside the system and the obtained voltage should provide more insight in this proof-of-concept, where a sinusoidal mechanical input shall convert to a constant output of electrical energy. All three sensors were connected to an Arduino that converted the sensed data into readable information. An Arduino is a micro-controller, that receives a voltage reading from the sensors and converts it to an output value through code that was created by the user. This script is uploaded to the board through the Arduino IDE software. Once the output data had been retrieved, it was transferred over to MATLAB or Excel, where a graphical representation of this data could be obtained.

6.1 Input regulator

When analyzing the results of an experiment, it is important that the input of that experiment is regulated in some kind. A well controlled input enables the experiment to be replicated, which enhances the credibility of the research (Nosek and Errington 2020). Therefore, an approach was sought to regulate the piston movement in the small-scale PTO.An ocean wave's exact profile is complex and cannot be described by a single sinusoidal wave. Instead, it consists of a combination of many different wave functions with different frequencies and amplitudes, as well as non-harmonic functions (Steele 1999). Nevertheless, this small-scale model is aiming to approach the dynamics of the large-scale system, and therefore, a basic sinusoidal wave input will suffice. A linear reciprocating mechanism is constructed in order to achieve linear movement along the vertical axis from a motor that produces circular motion (Metallidis and Natsiavas 2003). The design consisted of two rods connected to a disc, which was driven by a drilling machine. The disc was constructed out of HPL (High Pressure Laminate), a strong material that can withstand the forces that arise from rotating head of the drilling machine. A 3D printed crank was fitted with a bearing and connected to this disc, such that near frictionless rotation is allowed. On the other side of the crank, a metal rod was connected through another bearing. The metal rod served as a stabilizer for the plastic piston end, taking into account the high torque that can be produced by the drill.

Figure 28: Isometric view of the linear reciprocating mechanism.

Figure 29: Front view of the linear reciprocating mechanism.

Although the concept was fully functioning when tested, it was realised once again that the plastic tube, that served as the piston, would undergo such lateral forces that it would fracture quickly. The apparent solution included a conducting cylinder, constructed out of metal or PVC, that would force the piston to move in a vertical linear motion only. Considering the time span of the research, it was preferred to conduct the experiments first, and observe the consequences of the suboptimal human input force. Further research by Ocean Grazer B.V. could finish the linear reciprocating mechanism when required, as this subject could cover a study on its own.

6.2 Ultrasonic sensor

Without a controlled input mechanism, the accuracy of the human input force will also play a role in the reliability of the results of the experiments. The dynamics of the input force can be monitored by measuring the displacement of the piston with respect to a fixed point in the system. An ultrasonic sensor was used to determine this measure. The sensor functions by producing ultrasonic waves, that reflect upon objects that it comes across. The velocity of the wave is known, and therefore, the elapsed time for the wave to return back to the sensor is utilized to calculate the distance to the object.

Figure 30: The ultrasonic sensor that measures the distance between the lower end of the piston and the construction frame.

6.3 Force Sensitive Resistor

The force that is required to move the piston in a full stroke is measured using a Force Sensitive Resistor (FSR). This measuring device is a suitable alternative to a load cell, which is generally used in force sensing practices in large-scale applications. The FSR consists of a polymer layer that has a variable resistance between its terminals. When no force is applied on the film, the resistance of the sensor is larger than 1 MΩ. The sensor basically consists of many conducting particles that are as big as several micrometers. When an object is exerting force on the sensor, the particles touch, and the resistance of the sensor decreases rapidly. Following the datasheet of the Zunate RP-S40-ST FSR, the sensor actively produces an output when between 10 g and 10 kg of weight is placed onto the sensor.

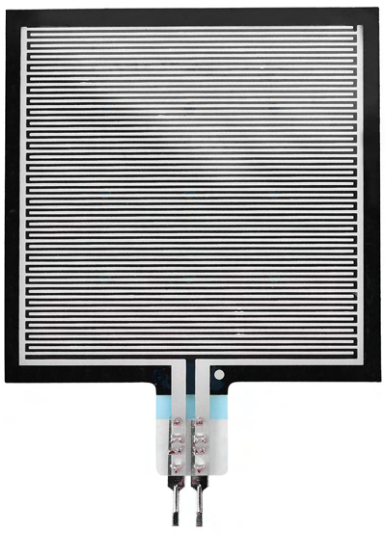

Figure 31: Top view of the Zunate RP-S40-ST Force Sensitive Resistor.

The RP-S40-ST FSR is connected to the Arduino Mega following the voltage divider circuit as given in in Figure 32. The Arduino micro-controller receives the output voltage V_{out}. R_0 is a resistor with known resistance, which is used to calculate R_s. From the datasheet, it is known that the relationship between R_s and the mass that is placed on the sensor is given by the equation 4.

$$R_s = 271.0{m_{in}}^{-0.69} \tag{4}$$

Derived using Ohm's law, the general equation for a voltage divider circuit is given by equation 5.

$$V_{out} = \frac{R_o}{R_s + R_0} V_{cc} \tag{5}$$

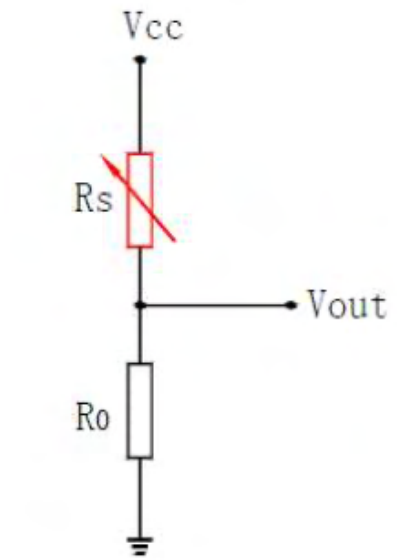

Figure 32: Circuit diagram of force sensitive resistor.

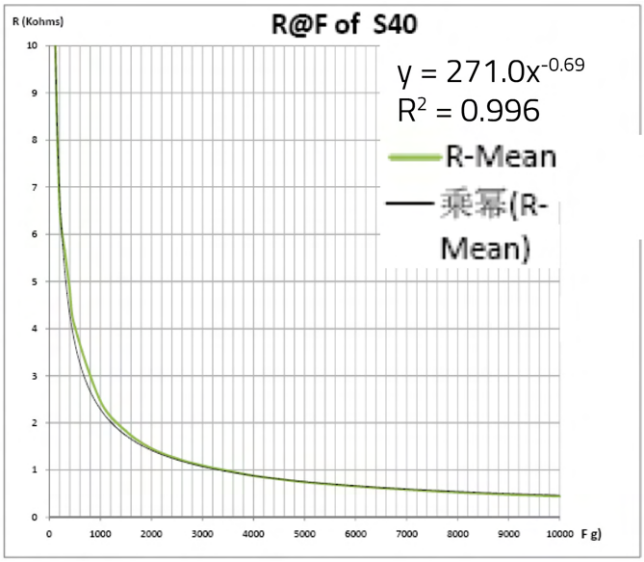

Figure 33: Graphical representation showing the relationship between resistance of the FSR and the input mass.

Rewriting equation 5 for R_s and gives:

$$R_S = R_0 \left(\frac{V_{cc}}{V_{out}} - 1 \right) \tag{6}$$

Substituting R_s from equation 4 into equation 6 and rewriting in terms of m_{in} leads to equation 7:

$$m_{in} = \left(\frac{271.0}{R_0 \left(\frac{V_{cc}}{V_{out}} - 1 \right)} \right)^{\frac{1}{0.69}} \tag{7}$$

Equation 7 proves to be very helpful in the measuring stage. With a known resistance value

R_0 and the input and output voltage values V_{cc} and V_{out}, the value of the mass that is placed on the sensor can be determined. The input voltage V_{cc} is given to be 5 V on the Arduino Mega microcontroller. Rewriting equation 7 for V_{out} in terms of m_{in}, substituting 5 V for V_{cc} and plotting the function for several values of R_0 results in the plot given in Figure 34. From this figure, it can be concluded that the choice of the resistance value R_0 influences the accuracy of the measurement for different ranges of mass inputs. If a high accuracy is desired in the low range of mass inputs, then a higher resistance is more appropriate, and similarly, a lower resistance value is a more suitable choice for large input masses. Following this conclusion, a resistance value of 1000 Ω has been chosen initially in order to get an accurate reading for a force that is expected to be in between 1-5 kg.

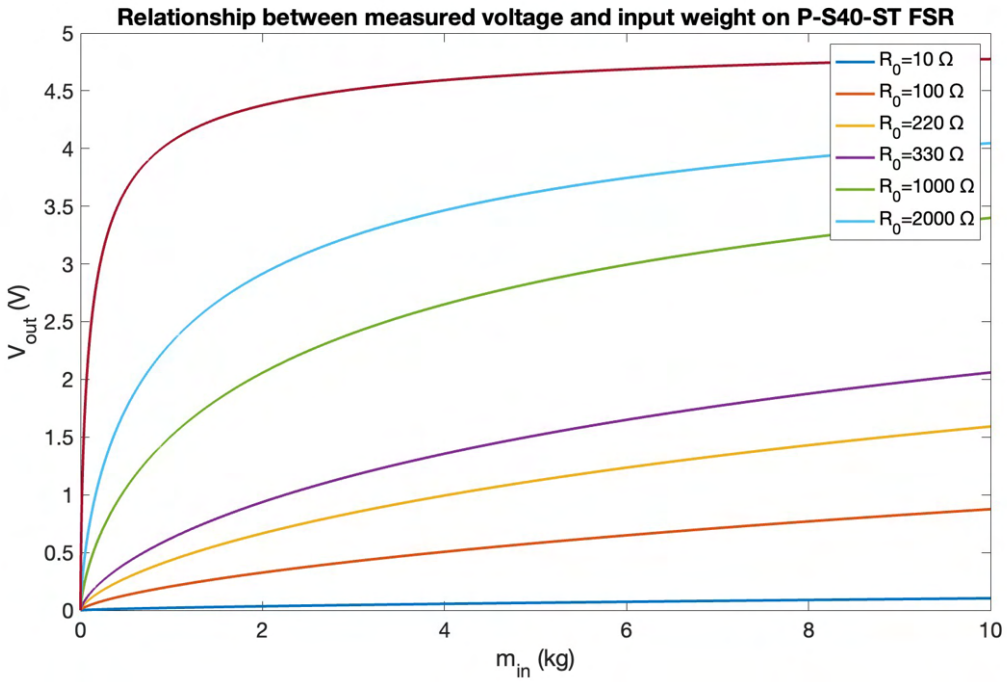

Figure 34: Graphical representation of the relationship between the measured voltage and the input weight on the P-S40-ST FSR.

The $40\,x\,40\,mm$ square bed of the P-S40-ST FSR was placed on a 3D printed mount from PLA, that could easily be connected to the end of the piston with one bolt. During testing, it was noticed that the FSR was fairly sensitive. Since force is calculated by multiplying the pressure and area, it is important that the area over which the force is applied remains constant. Therefore, another adapter was 3D printed from TPU filament, enabling the userto apply a force over the same area every time the piston was pushed upwards.

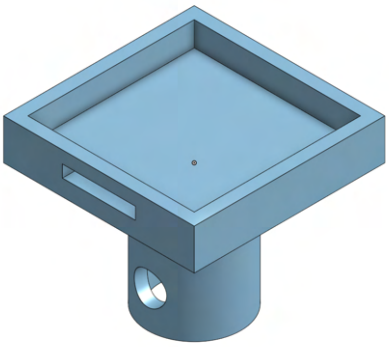

Figure 35: CAD model of the placeholder for the FSR.

Figure 36: The force sensing setup.

Once properly connected to the Arduino, it was quickly concluded that the sensor did not behave as described in equation 4, and the sensor had to be calibrated. Since the relationship between the input weight and the resistance of FSR was highly non-linear, it was decided to utilize MATLAB to process the calibration results in real-time, and perform a curve fitting operation using the function 'polyfit'. Pushing on the sensor with a scale underneath showed that the maximum deviation of the sensor was around 10% of the real weight. The datasheet confirms this relatively large error for such FSR sensors. As the measurement only aims to confirm whether a buoy in the wave flume might be able to move the piston, this error does not impose any problems for the usefulness of this experiment.

6.4 Pressure Transducer

Another experiment that executed on the small-scale PTO was a pressure measurement on the inlets of the cylinder. The aim of this experiment is to analyze the pressure difference between these two inlets, and conclude whether or not the up- and down stroke produce similar pressure levels on both sides of the system. The pressure measurement was taken using an industrially available pressure transducer, that is generally present in car engines for oil and fuel pressure measurements. Contrary to the FSR, this Kavlico P265 pressure transducer is much more accurate, with a maximum error of 2%.

Since the pressure transducer consisted of a tapered external 1/8" NPT (National Pipe Thread) thread instead of a more commonly used BSP thread, connecting the transducer required a different approach. Along with a 1/8" NPT T-piece, several NPT adapters were purchased to make a solid connection with the hose.

Figure 37: Several adapters were used to connect the P265 pressure transducer to the circuit.

The pressure sensor was available in a different range options, with the upper pressure limit ranging from 30 PSI to 100 PSI. Since only small pressure values were expected, and a relatively high accuracy was required, the 30 PSI version was chosen for this experiment. It is known that this sensor has a voltage output between $0,5V$ and $4,5V$, and the response is linear in relationship with measured the pressure, making the calibration of the sensor relatively straightforward. The signal of the sensor was transmitted to the Arduino via one of its analog connection pins.

6.5 Voltage Sensor

In order to measure whether the PTO is actually able to turn mechanical energy into electrical energy, a voltage sensor was attached to the hydro generator. Before connecting the generator directly, it is important to note that the input pins on the Arduino can handle up to $5\,V$. Considering that the hydro generator should be able to produce a $12\,V$ output when running at full velocity, a specific sensor was required for this measurement to prevent the Arduino from becoming defective due to overvoltage. Therefore, an Akozon voltage sensor was purchased that is able to give an accurate voltage reading from power delivery devices up to $25\,V$. The sensor was programmed similarly to the pressure transducer in the Arduino IDE software.

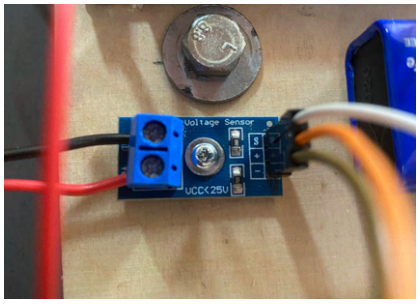

Figure 38: The Akozon voltage sensor embedded in the circuit.

7 Results

The outcomes of the experiments that were executed in the last paragraph will be outlined in this section. The displacement, pressure and voltage measurements have been performed simultaneously. Their results have been processed in Microsoft Excel. The force experiment had been executed before in identical conditions, since the setup for measuring force and displacement both required the end of the piston to be free. The force measurements were processed in Matlab.

7.1 Displacement

In 6 seconds, the piston completes 6 periods of oscillation, meaning that the frequency is exactly $1\,Hz$ ($f = \frac{1}{T}$). The average amplitude is approximately 7,5 centimeters, which results in a full piston stroke of 15 centimeters. Note that the piston is in its downstroke when the displacement increases due to the postion of the ultrasonic sensor.

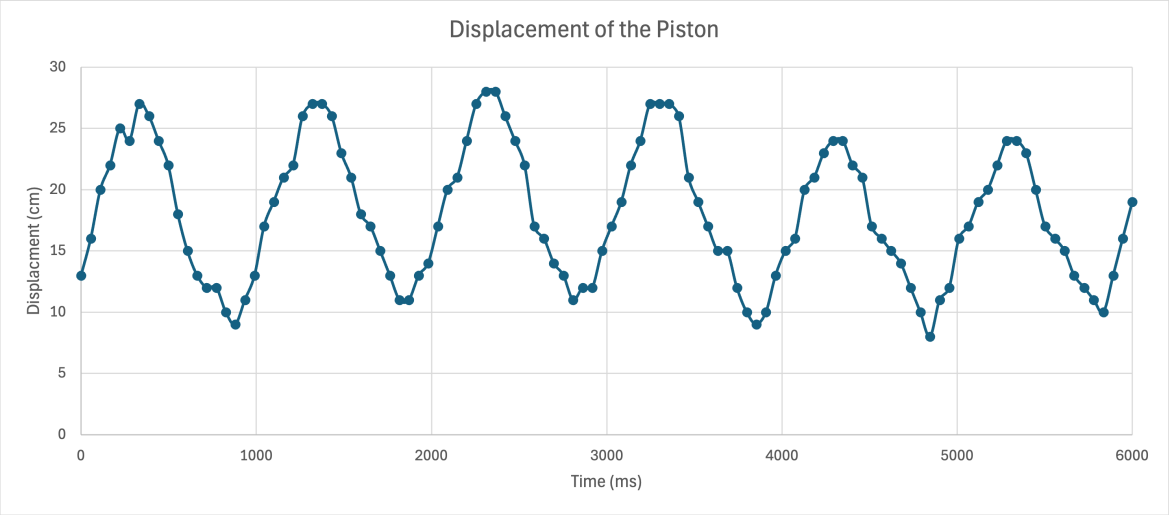

Figure 39: Graphical representation displacement of the piston end, relative to the bottom of the wooden frame.

7.2 Force

The resulting graph from the force measurements shows that the initial force that is required to get the system running is $33,85\,N$. In a sequence of 10 cycles and 7,5 seconds in which the piston moves up and down, the maximum force that is observed is $25,03\,N$. In the downstroke, the piston is being pulled upon, and no force is registered by the sensor.

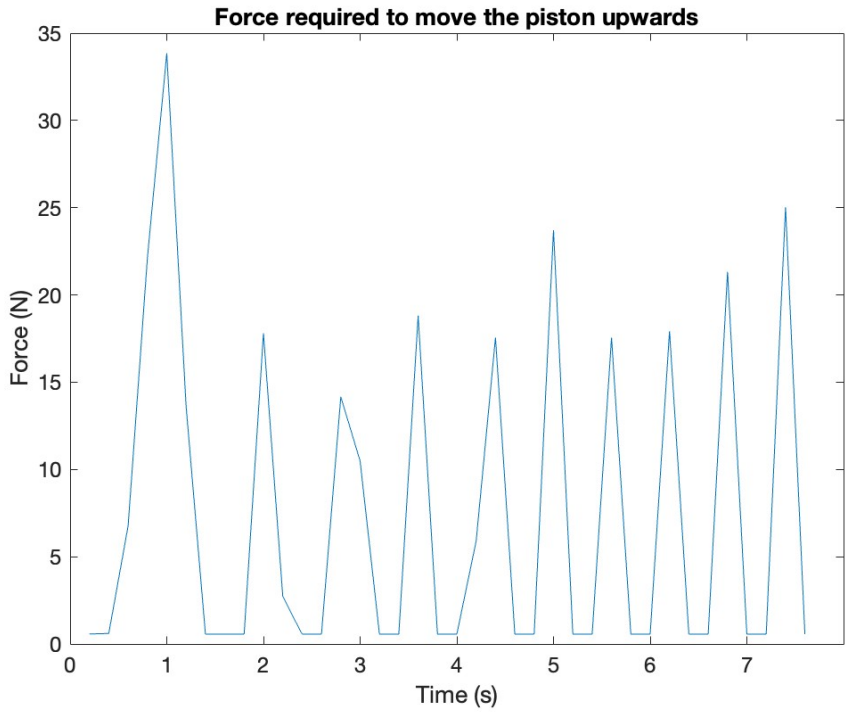

Figure 40: Graphical representation of the force required to move the piston upwards, measured using the P-S40-ST FSR.

7.3 Pressure

In the combined graph of the pressure measurements at both inlets it is found that the maximum pressure for the upper inlet is $10,0\,PSI$, and the minimum pressure is $-3,7\,PSI$. For the lower inlet, the maximum pressure is $9,9\,PSI$ and the minimum pressure is $-1,5\,PSI$. The phase shift between the two graphs is π radians. Similarly to the displacement measurements, the frequency is $1\,Hz$.

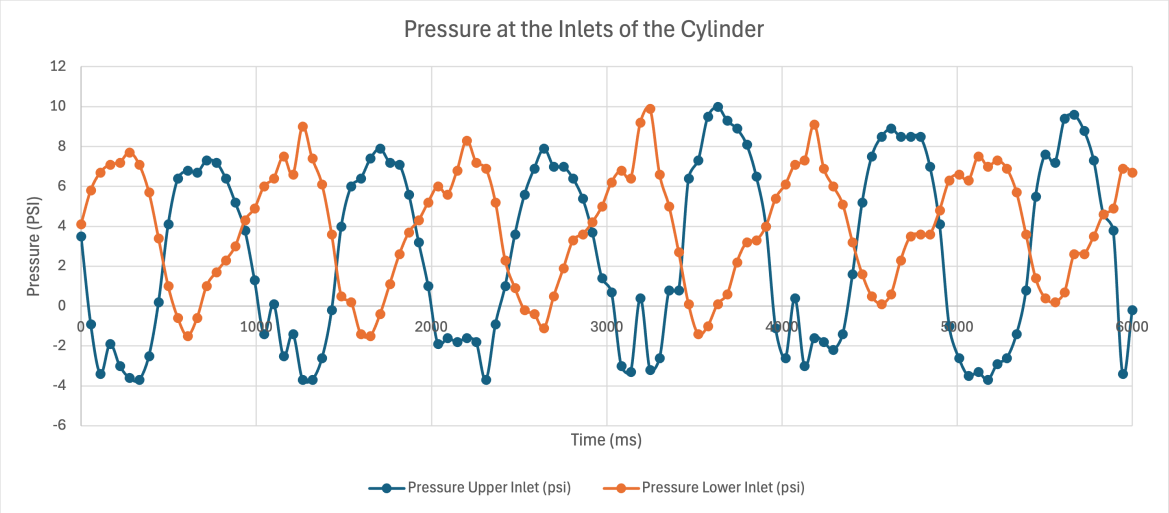

Figure 41: Graphical representation of pressure measured at both inlets of the cylinder.

7.4 Voltage

The voltage graph of the hydro generator shows a variable output, with a noticable amount of datapoints located on the horizontal line that resembles a $12\,V$ output. The highest voltage that has been measured is $12,11\,V$, while the lowest voltage that has been captured is $3,74\,V$.

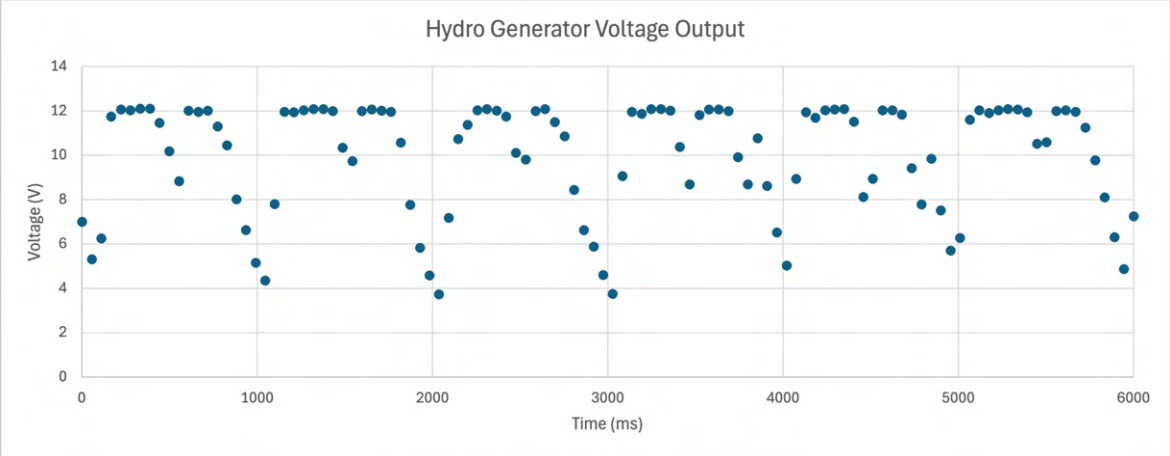

Figure 42: Graphical representation of voltage output of the hydro generator.

7.5 Combined Graph

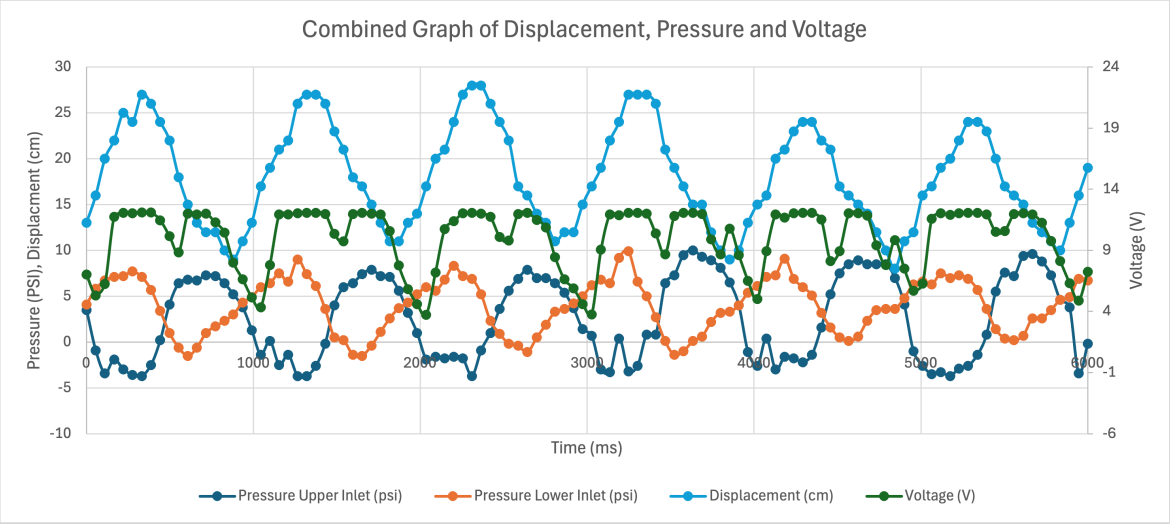

Figure 43: Graphical representation of the displacement of the piston, the pressure at both inlets of the cylinder and the voltage output of the hydro generator, combined into one figure.

8 Discussion

8.1 Displacement

From the displacement graph that has been recorded using the ultrasonic sensor, it is noticed that the shape of the figure resembles a sinusoid relatively well, as desired. During the last 2 seconds of the recorded data, the range of the pistons movement is shifted up by around 3,5 centimeters, due to human error. It would be interesting to see what effect having a perfect sinusoid as input would have on the resulting sinusoidal graphs that have been obtained. It is expected that these graphs would smooth out when this human error is removed. Nevertheless, in the ideal situation an ocean wave would drive the PTO, with all its imperfections. The construction of a conducting cylinder out of metal or PVC would certainly improve the performance of the small-scale PTO, by enabling the possibility of a regulated input or a wave tank implementation, although a revised design of the buoy would be required in addition. Looking at the range, the hydro generator would be able to function properly within the wave flume, as it is tested running completely up to standards with a a stroke of around 15 centimeters.

8.2 Force

The force of $33,85\,N$ for an initiation of the PTO and $25,03\,N$ for an upstroke in the middle of a wave sequence seem reasonable, both for a human input and an actual scenario where a wave drives the PTO. It is assumed that these forces are similar for the downstroke, since no difference was felt in the power that was required to push or pull the piston.
Highly simplified, the movement of a wave consists of an upward and downward motion. A floating object that finds itself in the downward motion is mainly impacted by the gravitational force that pulls the object to towards the seabed. The gravitational force on the object on earth is given by:

$$F_g = mg \tag{8}$$

Where F_g is the gravitational force that is experienced by an object on earth, m is the mass of that object and g is the constant of acceleration due to gravity, which is approximately 9,81. This means that F_g shall be more than $33,85\,N$ in order to pull the piston down. Otherwise, the object will stay attached to the end of the piston en decouple from the water's surface. In the upward motion of the wave, a floating object is mainly influenced by the buoyancy force. This force is given by Archimedes' Principle, which states that the buoyancy force is equal to the weight of the water that is displaced by the object:

$$F_b = \rho_f g V \tag{9}$$

Where F_b is the buoyancy force, ρ_f is the density of the fluid, g is the acceleration due to gravity and V is the volume of the submerged object.
When the buoyancy force is equal to, or greater than the gravitational force, an object will be kept afloat. A force balance can be set up for this situation:

$$\uparrow \sum F = \rho_f g V - mg \tag{10}$$

Which can be simplified to:

$$m = \rho_f V \tag{11}$$

The density of fresh water at room temperature ($20°C$) is measured to be $998.2072\,kg/m^3$, representing the scenario in the wave tank. Sea water, with an increased salinity, has a higher density, which is recorded to be $1024.8103\,kg/m^3$ under similar circumstances (ITTC 2011).

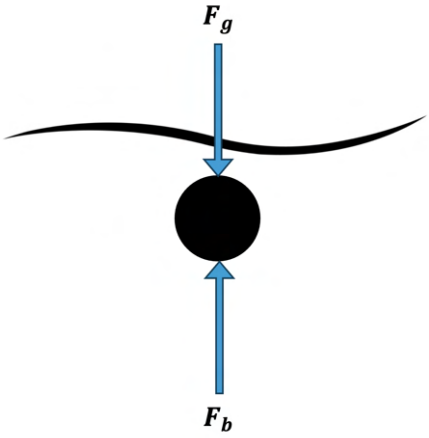

Figure 44: Force balance of an object that is fully submerged.

Under the condition of equation 11, the object that is submerged finds itself in an equilibrium condition, and it will just stay afloat. The floater that should be used in combination with the PTO system in the wave tank should comply with two constraints:

$$\begin{cases} F_b - F_g \geq 33,85\,N \\ F_g \geq 33,85\,N \end{cases}. \tag{12}$$

These equations state that a floater with a given volume, should have a minimum mass, such that the difference between the buoyancy force and the gravitational force is greater than, or equal to the required 33,85 N (condition 1). Additionally, the mass of the floater should be large enough such that the gravitational force exceeds the force that is required to move the piston downwards (condition 2). In practice, this means that for the scenario in the wave tank,

assuming that a floater of minimum mass is preferred, the following characteristics hold:

$$9,81 m_{min} = 33,85 \tag{13}$$

$$m_{min} = 3,45... \, kg \tag{14}$$

For this situation, equation 12 is used to find the minimal volume that is required for the object:

$$\rho_f g V - m_{min} g \geq 33,85 \tag{15}$$

$$\rho_f V - m_{min} \geq \frac{33,85}{9,81} \tag{16}$$

$$V \geq \frac{3,45... + 3,45...}{998.2072} = 6,91... \times 10^{-3} m^3 \tag{17}$$

Therefore, the minimal weight the floater must have is approximately $3,45\,kg$, and the corresponding minimal volume is $6913\,cm^3$. A $20\,x\,20\,x\,20\,cm$ acrylic cube, with a volume of $8000\,cm^3$, similar to to one that has previously been used as a floater inside the wave tank, could be used again for this purpose. Even so, the connection point of the floater to the piston must be designed for this system specifically. The 10% error that is associated with the FSR as mentioned before should be taken into account when designing a floater for this PTO.

8.3 Pressure

The pressure readings of the PTO show two out of phase graphs for both the upper and lower cylinder inlets. Remarkably, the positive upper pressure limits of the graph are generally much higher than the lower limits of the graph, in abstract sense. This indicates that a larger body of water is pushed out of the cylinder than that which is pulled back inwards. This may be caused by the fact that either water is left behind in the tubing, or water is leaking out of the system. Since any severe leakages were eliminated beforehand, the first reason seems more evident. Furthermore, it has been noticed that although the upper pressure values are almost identical for both the upper and lower cylinder inlets, their lower pressure limits deviate. For the upper inlet, the lower pressure limit is much smaller than for the bottom inlet. This can be elaborated by the fact that in the bottom pressure inlet, fluid has to move upwards into the cylinder, against the gravitational force. It can be concluded that filling up not only the cylinder, but also all tubing in the system with water, can greatly reduce the lower pressure limit of the system, and thus the overall performance.

8.4 Voltage

The voltage output of the hydro generator shows that it is only capable of producing a constant $12\,V$ output when running above a certain base level. From the combined graph, it is noticed

that the voltage drops occur repetitively when the pressure at the lower inlet s increasing, indicating that the down stroke of the cylinder is less powerful than the upstroke of the cylinder. Gravitational forces can again be held responsible for this observation, since water must be pumped upwards from the lower inlet before it reaches the hydro generator. Only when the system is completely filled up with fluid, this effect is reduced. It is also expected that accumulators, which are normally present in the large-scale systems, could even out the voltage production. Further research could look into the addition of accumulators into the system.

9 Conclusion

The design and development of a small-scale PTO for a wave energy converter yielded promising results. Aiming to simulate the dynamics of the large-scale system in the best way possible, a similar circuit to that of a full scale hydraulic PTO was designed. However, since it was found that the magnitude of forces in the aforementioned system do not scale down with the size of the parts in the system proportionally, a different approach of using more off-the-shelf components was taken. In the second design cycle, the elements that were forming a bottle neck for smooth flow within the system, such as the check valves, were replaced for industrially available components, which significantly enhanced the performance of the system. The results from experiments involving displacement, force, pressure and voltage measurements proved the PTO's capability turn the mechanical energy provided by a vertically moving floater, into electrical energy by running a hydro generator. A relatively constant voltage output was recorded, with a number of remarkable drops at sequential intervals. Pressure measurements indicated a possible cause for the issue, showing that the voltage drop occurred during every downstroke, where water was travelling against gravity. This result highlighted the importance of a fully loaded system. Furthermore, the measurements of a force sensitive resistor showed that at least $33,85\,N$ of force was required to initiate the system, which is well to be done by the floater that is currently available in the wave flume. Future work should focus on a certain type of input regulation, whether by using a floater in the wave tank, or a reciprocating mechanism. Furthermore, accumulators could be integrated to smooth out voltage production. Overall, the project provides a valuable proof-of-concept, that can well be refined in order to validate numerical models from other researches. Thereby, the design sets another step forward to realising a fully sustainable energy production in the future.

References

Bjerke, May Britt and Ralph Renger (2017). "Being smart about writing SMART objectives". In: *Evaluation and Program Planning* 61, pp. 125–127. ISSN: 0149-7189. DOI: https://doi.org/10.1016/j.evalprogplan.2016.12.009. URL: https://www.sciencedirect.com/science/article/pii/S0149718916302580.

Drew, Benjamin, Andrew R Plummer, and M Necip Sahinkaya (2009). *A review of wave energy converter technology*.

Fernández Vuelta, Adrián (2017). "Modular modelling for the power take-off system of a wave energy converter". MA thesis. Universitat Politècnica de Catalunya.

Hassink, MA (2016). "Design of experimental measurements to obtain performance characteristics of a multiple ball check valve". PhD thesis. Faculty of Science and Engineering.

Henderson, Ross (2006). "Design, simulation, and testing of a novel hydraulic power take-off system for the Pelamis wave energy converter". In: *Renewable energy* 31.2, pp. 271–283.

Home — oceangrazer.com (n.d.). https://oceangrazer.com. [Accessed 12-03-2024].

ITTC, 26th (2011). *7.5-02-01-03 fresh water and seawater properties*. URL: https://www.ittc.info/media/7989/75-02-01-03.pdf.

Jusoh, Mohd Afifi et al. (2019). "Hydraulic power take-off concepts for wave energy conversion system: A review". In: *Energies* 12.23, p. 4510.

McLean, Niall et al. (2023). "Multi wave absorber platform design, modelling and testing: Investigating the integration of multiple wave energy absorbers into a floating offshore wind platform considering a future wind and wave energy hybrid system". In: *Proceedings of the European Wave and Tidal Energy Conference*. Vol. 15.

Metallidis, P and S Natsiavas (2003). "Linear and nonlinear dynamics of reciprocating engines". In: *International Journal of Non-Linear Mechanics* 38.5, pp. 723–738.

Nosek, Brian A and Timothy M Errington (2020). "What is replication?" In: *PLoS biology* 18.3, e3000691.

Nur, A, R Afrianita, and RDTF Ramli (2019). "Effect of pipe diameter changes on the properties of fluid in closed channels using Osborne Reynold Apparatus". In: *IOP Conference Series: Materials Science and Engineering*. Vol. 602. 1. IOP Publishing, p. 012058.

Peña-Sanchez, Yerai, Demián García-Violini, and John V Ringwood (2022). "Control co-design of power take-off parameters for wave energy systems". In: *IFAC-PapersOnLine* 55.27, pp. 311–316.

Penalba, Markel et al. (2017). "Validating a wave-to-wire model for a wave energy converter—Part I: The Hydraulic Transmission System". In: *Energies* 10.7, p. 977.

Shadman, Milad, Gustavo Omar Guarniz Avalos, and Segen F Estefen (2021). "On the power performance of a wave energy converter with a direct mechanical drive power take-off system controlled by latching". In: *Renewable Energy* 169, pp. 157–177.

Steele, KE (1999). “Ocean wave heave time series as the sum of nonharmonic sinusoids”. In: *Ocean engineering* 26.12, pp. 1335–1357.

Stram, Bruce N (2016). “Key challenges to expanding renewable energy”. In: *Energy Policy* 96, pp. 728–734.

Takao, Manabu, Toshiaki Setoguchi, et al. (2012). “Air turbines for wave energy conversion”. In: *International Journal of Rotating Machinery* 2012.

Têtu, Amélie (2017). “Power take-off systems for WECs”. In: *Handbook of ocean wave energy*, pp. 203–220.

Verschuren, Piet, Hans Doorewaard, and Michelle Mellion (2010). *Designing a research project*. Vol. 2. Eleven International Publishing The Hague.

Wieringa, Roel and Ayşe Moralı (2012). “Technical action research as a validation method in information systems design science”. In: *International Conference on Design Science Research in Information Systems*. Springer, pp. 220–238.

Xu, Tao et al. (2020). “Mechanical properties of additively manufactured thermoplastic polyurethane (TPU) material affected by various processing parameters”. In: *Polymers* 12.12, p. 3010.